Mobility of electrons in a quasi-one-dimensional conducting channel on the liquid-helium surface

Sviatoslav S. Sokolov
Departamento de Física, Universidade Federal de São Carlos, 13565-905, São Carlos, São Paulo, Brazil and B. I. Verkin Institute for Low Temperature Physics and Engineering, Academy of Sciences of Ukraine, 310164, Kharkov, Ukraine

Guo-Qiang Hai and Nelson Studart
Departamento de Física, Universidade Federal de São Carlos, 13565-905, São Carlos, São Paulo, Brazil
(Received 11 October 1994)

The mobility of electrons in a quasi-one-dimensional channel on the surface of liquid helium is studied theoretically at temperatures lower than 1.5 K. The influence on the mobility due to the electron-ripplon interaction and to the electron scattering from helium atoms in the vapor phase is investigated. The nonmonotonic temperature dependence of the mobility below 0.5 K is attributed to the contribution coming from the matrix elements of the scattering operators between different subbands due to the confinement of the electron motion along the channel. It is shown that the results taking electron-electron correlations into account in the complete control approximation differ significantly from the results in the usual one-electron approximation. This allows us to check the role of electron correlations in quasi-one-dimensional electron systems by comparing the theoretical temperature dependence of the mobility with the experimental data.

I. INTRODUCTION

During the last decades the studies of low-dimensional charge systems became one of the most interesting and rapidly developing topics in the physics of systems with reduced spatial dimensionality. Two-dimensional (2D) charge systems, where electrons are free to move in the plane, but are confined in the third spatial direction, are realized in semiconductor structures and on the surface of dielectrics, especially on the surface of liquid helium. The well-known 2D electron systems cover wide range of electron densities, leading to examples either of quasi-two-dimensional degenerate charge systems in semiconductor heterostructures[1] or of classical systems of surface electrons (SE's) over liquid helium.[2]

Recently the great technological progress in crystal growth, lithography, and etching processes has led to the fabrication of semiconductor structures where charge carriers are free to move only in one spatial direction due to lateral confinement and forming a quasi-one-dimensional (Q1D) charge system. A lot of interesting effects have been investigated both theoretically and experimentally in these Q1D degenerate electron systems including transport[3] and optical properties,[4] resonant tunneling,[5] many-body effects and plasmon excitations,[6] the role of impurities,[7] the peculiarities of the electron-phonon interaction,[8] and so on.

The intensive study of Q1D charge systems in semiconductors motivated the search for creating a similar Q1D electron system based on the SE's on liquid helium. Such a system would have all the advantages, which are typical for SE systems, like cleanness, homogeneity, and the possibility of a wide variation of the experimental parameters such as the electron concentration, thickness of the helium film, and the clamping electric field. In this sense, the physical realization of this system should open the possibility to study different phenomena in the Q1D classical electron system.

A proposal for the experimental realization of a Q1D electron system on the surface of liquid helium was made by Ginzburg and Monarkha.[9] They suggested to use a special dielectric substrate with a triangular profile on the surface in the same way as a diffraction grating. When the substrate is covered with superfluid helium, the electrons will be concentrated along the top of the linear grooves of the grating due to the large image forces from the substrate acting on the electrons. Attempts to realize the proposed system[10] demonstrated, however, that, at liquid depths over the ridges around 10^{-5} cm, where the role of the substrate on the electrons is dominant, it is very difficult to avoid the influence of defects of the substrate surface which sizes are of the same order of magnitude of the liquid depth. It was also suggested by Chaplik[11] that a Q1D electron system can be created by positively charging thin metallic wires located under the helium surface. Unfortunately, up to now there is no experimental evidence of the physical realization of these proposals probably due to difficulties for creating reliable conditions of good enough homogeneity of the system.

In 1986, Kovdrya and Monarkha[12] proposed another way to create the Q1D electron system using the finiteness of the curvature radius of the liquid in parallel channels on the surface of a dielectric substrate with linear grooves. These channels are filled by superfluid helium under the action of the capillary forces. A sketch of the geometric arrangement of the system is shown in Fig. 1. If the substrate is located at the height H above the level of bulk liquid helium, the curvature radius of the helium

0163-1829/95/51(9)/5977(12)/$06.00

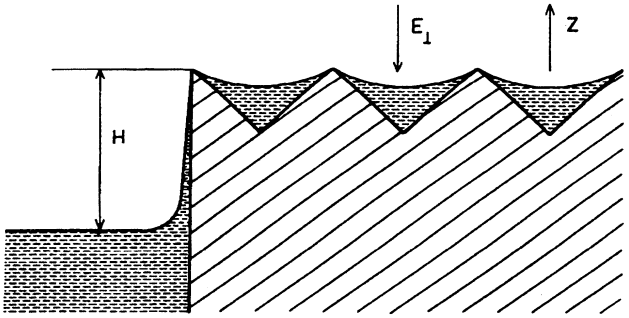

FIG. 1. The scheme of the realization of quasi-one-dimensional electron system over liquid helium Ref. 10. The natural depth of helium film is enhanced.

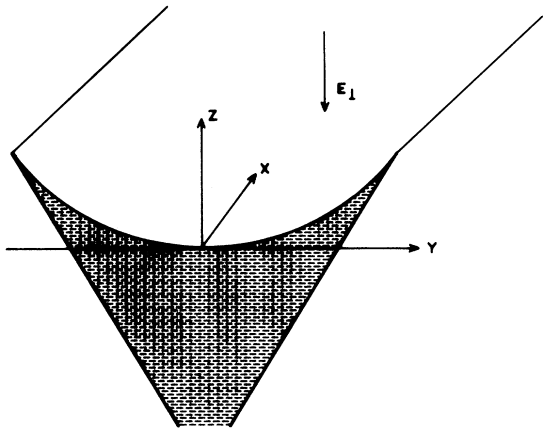

FIG. 2. The cross section of the channel filled by liquid helium between two dielectric planes. Electrons are localized along the x axis; the holding field $E_\perp$ is along the z axis.

surface is given by

$$R = \frac{\alpha}{\rho g H} \quad , \tag{1}$$

where α and ρ are the surface tension and the helium density, respectively, and g is the acceleration due to gravity. As in the previous case, when the helium surface over the dielectric substrate with the linear grooves is charged by a heated filament, the polarizing forces from the substrate try to concentrate the electrons over the ridges. However, when the holding electric field $E_\perp$, along the z axis, is switched on, the electrons are shifted to the bottom of the channel, concentrating mainly along the x axis. Now, the electrons are located at large distances from the substrate because the normal size of the curvature radius $R \simeq 10^{-4}$–10^{-3} cm is much larger than the size of substrate inhomogeneities ($\sim 10^{-6}$–10^{-5} cm) and the liquid depth below the electron channel is of the same order as R. So the influence of the substrate roughness on the electron gas is negligible, and the Q1D electron system should be very pure and homogeneous, as the SE's on bulk helium, and could exhibit high mobilities. The experimental realization of this situation was made by Kovdrya and Nikolaenko[13] who show explicitly the strong anisotropy of the electron conductivity along and across the series of channels filled with superfluid helium. Recently, Kirichek *et al.*[14] described a simple method for creating a solitary channel of high-mobility electrons on a helium surface strongly distorted by capillary forces due to a substrate formed by two dielectric polymer sheets meeting at a sharp angle, as shown in Fig. 2. In this approach, the profile of the helium surface and the conditions to create the Q1D electron system are the same as in the previous works.[12,13] But contrary to the proposal described in Ref. 12 and experimentally realized in Ref. 13, there is no interaction between the electrons in adjacent channels, and just only one channel is formed. The previous experimental study in Ref. 14 demonstrated that the electron conductivity along the channel has a nonmonotonic dependence on the holding field.

As is known the study of SE's kinetics gives the possibility to investigate not only the interaction between the carrier and scatter but also the influence of interparticle correlations in the transport process.[15] It is expected that correlation effects in the Q1D electron system with one less degree of freedom are more important than in the 2D case. Furthermore, the Q1D character of the electron motion leads to another structure of the matrix elements of the scattering potential in comparison with the case of SE's.[16] As a result, one can obtain other temperature and field dependences of the kinetic coefficients. For these reasons, a detailed and consistent theoretical and experimental study of the transport properties of the Q1D electron system in the conducting channel over the liquid surface seems to be of current interest. The aim of the present work is to study the electron mobility in such a Q1D system based on linear response theory and the Boltzmann equation. The electron mobility will be calculated within the usual one-electron approximation and the complete control approximation[15] depending on the contribution of electron-electron scattering.

The paper is organized as following. In Sec. II, we will give a brief description of the electron states in the conducting channel. In Sec. III, the transport equation of the Q1D electron gas is presented including the scattering mechanisms of the ripplons, and the helium atoms in the vapor phase, as well as the electron-electron interaction. The electron mobility is evaluated within the one-electron approximation when electron-electron scattering can be neglected, and within the complete control approximation where electron-electron scattering is pronounced and is effectively taken into account in an indirect way. A comparison of the mobility in the two approximations considered is also presented. Our conclusions are summarized in Sec. IV.

II. ELECTRON STATES IN THE Q1D CHANNEL

The conducting channel filled with liquid helium is represented schematically in Fig. 2. The profile of the liquid surface is close to a semispherical form and can be described by the equation

$$z = R\left(1 - \sqrt{1 - \frac{y^2}{R^2}}\right) \simeq \frac{y^2}{2R} \quad \text{for } y \ll R\,. \tag{2}$$

The holding field $E_\perp$ is applied in the z direction. If an electron at the bottom of the channel moves a distance y from the center, it is subjected to a potential

$$U(y) = \frac{m\omega_0^2 y^2}{2}, \tag{3}$$

which laterally confines the electron in the y direction with characteristic frequency $\omega_0 = \sqrt{eE_\perp/mR}$, where m and e are the electron mass and charge, respectively. Due to such a parabolic confinement potential, the motion of the electron in this direction is quantized. The corresponding eigenenergy and the wave function are given by

$$\epsilon_n = (n + 1/2)\hbar\omega_0, \qquad n = 0, 1, 2, \ldots, \tag{4}$$

and

$$\varphi_n(y) = \frac{1}{\pi^{1/4} y_0^{1/2}} \frac{1}{\sqrt{2^n n!}} \exp\left(-\frac{y^2}{2y_0^2}\right) H_n\left(\frac{y}{y_0}\right), \tag{5}$$

respectively, where $y_0 = \sqrt{\hbar/m\omega_0}$ is the localization length in the y direction, and $H_n(x)$ is the Hermite polynomial. Typical values of y_0 along with the corresponding values of ω_0 are presented in Table I. As one can see from this table, the values of y_0 satisfy well the condition $y_0 \ll R$ for holding fields $E_\perp \approx 10^2$–10^3 V/cm. Moreover, for the root mean square of the electron displacement with $n > 0$, the inequality

$$\sqrt{\langle y_n^2 \rangle} = \left(n + \frac{1}{2}\right)^{\frac{1}{2}} y_0 \ll R \tag{6}$$

is satisfied even for $n \leq 10^2$. So the parabolic approximation of the confinement potential in Eq. (3) is rather good for the description of the electron motion along the y axis in a wide range of holding field $E_\perp$ and quantum number n.

Because the electron can move freely in the x direction, its total energy and wave function can be written as

$$E_{n,\,l}(k_x) = \frac{\hbar^2 k_x^2}{2m} + \epsilon_n + \Delta_l \tag{7}$$

and

$$\Psi_{n,\,l,\,k_x} = \frac{1}{\sqrt{L_x}} \exp(i\,k_x x)\,\varphi_n(y)\chi_l(z), \tag{8}$$

TABLE I. The parameters characterizing the electron localization in the Q1D channel filled by liquid helium with $R = 5 \times 10^{-4}$ cm.

$E_\perp$ (V/cm)	y_0 (10^{-6} cm)	$\hbar\omega_0$ (K)
450	5.4	0.3
900	4.5	0.4
2000	3.7	0.64
3000	3.35	0.8

respectively, where Δ_l and $\chi_l(z)$ indicate the electron eigenenergy and wave function in the z direction with index $l = 1,2,3,\ldots$, k_x is the electron wave vector, and L_x is the size of the system in the x direction. The mean distance of the electron from the surface in the ground state ($l = 1$) is $\langle z \rangle_1 = 114$ Å at $E_\perp = 0$ and is smaller for $E_\perp \neq 0$. So the condition $\langle z \rangle_1 \ll R$ is satisfied and the wave function $\chi_l(z)$ and the eigenenergy Δ_l can be taken as in the case of a flat helium surface approximately. For $E_\perp \geq 300$ V/cm, one can neglect the electron transitions from the ground level $l = 1$ at temperatures $T \lesssim 2$ K. In such a case, we consider

$$\chi_1(z) = 2\gamma^{3/2}\, z\, e^{-\gamma z} \tag{9}$$

for $z > 0$, where parameter γ is dependent on $E_\perp$ and is determined variationally.[17]

One should note that Eqs. (7) and (8) are valid for smaller holding fields than those given in Table I as long as $y_0 \ll R$. However, the minimum energy $eE_\perp R$ to confine the electron near the bottom of the channel must exceed the typical value $E_b \sim 10^2$ K of the binding energy of the electron on a superfluid helium film covering the dielectric plates which form the channel.[12] For this reason, we consider only the holding field $E_\perp > 300$ V/cm such that the condition $eE_\perp R \gg E_b$ is fulfilled for $R \sim 10^{-4}$–10^{-3} cm.

III. ELECTRON MOBILITY

The description of the Q1D electron states given by Eqs. (7) and (8) was proposed in Ref. 12, and the transport properties of the electrons were also studied theoretically in the quantum limit approximation; i.e., only the occupation of the lowest subband was considered. Such an approximation is realized in the system with low electron density at temperatures $T \ll \hbar\omega_0$. However, the typical temperature, where the experiments are performed, is around 1 K and the energy difference $\hbar\omega_0$ between the adjacent subbands is comparable to the thermal energy (see Table I). Obviously, the effect of the higher subbands has to be considered in the calculation of the electron mobility in the present system, where not only intrasubband scattering but also intersubband scattering processes are important for the electron transport.

The main scattering mechanisms for electron transport on the surface of liquid helium are the scattering by surface excitations of superfluid helium (ripplons) and helium-atom scattering in the vapor phase. The former dominates the electron mobility when $T \lesssim 1$ K, and the latter is the most important scattering mechanism for higher temperature $T \gtrsim 1$ K. For finite electron density, the scattering between electrons can also play an important role and must be included in the Boltzmann equation. Keeping these in mind, the Boltzmann equation governing the transport properties of electrons in the Q1D channel on the helium surface can be written as

$$\frac{\partial f_n}{\partial t} + \frac{eE_\parallel}{\hbar}\frac{\partial f_n}{\partial k_x} = \widehat{S}_{er}\{f_n\} + \widehat{S}_{eg}\{f_n\} + \widehat{S}_{ee}\{f_n\}, \tag{10}$$

where $E_\parallel$ is the driving electric field along the x direction,

f_n is the distribution function of electrons in the nth subband, and $\hat{S}$ represents the collision operator which is a functional of f_n. For electron-ripplon scattering the collision integral is given by

$$\hat{S}_{er}\{f_n\} = \frac{2\pi}{\hbar S}\sum_{n',q_x,q_y}|\langle n'|e^{iq_y y}|n\rangle|^2|\langle 1|V_q(z)|1\rangle|^2 \times\left\{[(N_q+1)f_{n'}(k_x+q_x)-N_q f_n(k_x)]\,\delta\left(\epsilon_{n'}-\epsilon_n+\frac{\hbar^2}{2m}(q_x^2+2k_xq_x)-\hbar\omega_{rq}\right)\right. \left.+[N_q f_{n'}(k_x+q_x)-(N_q+1)f_n(k_x)]\,\delta\left(\epsilon_{n'}-\epsilon_n+\frac{\hbar^2}{2m}(q_x^2+2k_xq_x)+\hbar\omega_{rq}\right)\right\}, \quad (11)$$

where $N_q = [\exp(\hbar\omega_{rq}/T)-1]^{-1}$ is the number of the ripplons with energy $\hbar\omega_{rq}$, $\vec{q}$ is the two-dimensional wave vector of the ripplon, and S is the area of the liquid surface. $V_q(z)$ in the above equation is the Fourier transform of the electron-ripplon interaction potential,[16]

$$V_q(z) = \left(\frac{\hbar q}{2\rho\omega_{rq}}\right)^{1/2}\left\{\frac{\Lambda_0 q}{z}\left[\frac{1}{qz}-K_1(qz)\right]+eE_\perp\right\}, \quad (12)$$

where $\Lambda_0 = (e^2/4)(\varepsilon_{\rm He}-1)/(\varepsilon_{\rm He}+1)$, $\varepsilon_{\rm He} = 1.057$ is the dielectric constant of helium, $\omega_{rq} = (\alpha/\rho)^{1/2}q^{3/2}$ the ripplon dispersion relation, α the surface tension, ρ the helium density, and $K_1(qz)$ the modified Bessel function. We have assumed that, in Eq. (12), the thickness of the helium film underneath the electrons is infinite.

By analyzing the transition matrix elements, we find $|\langle n'|\exp(iq_y y)\ |n\rangle|^2 \sim \exp(-q_y^2 y_0^2/2)$. It implies that the main contribution to the scattering process comes from the ripplons with $q_y < y_0^{-1}$, which corresponds to $q_y \lesssim 10^5$ cm^{-1} (see Table I). The same estimate for typical values of q_x can be made from the analysis of the energy conservation constraints given by the arguments of the δ functions in Eq. (11). So one can conclude that the characteristic wave number of ripplons in Eq. (11) satisfies the condition $q \lesssim 10^5$ cm^{-1} at temperatures around 1 K. For q in this region, the ripplon energy $\hbar\omega_{rq} \sim 10^{-3}$ K is negligible in comparison with the typical electron energy which is of the order of the thermal energy. With this consideration, Eq. (11) reduces to

$$\hat{S}_{er}\{f_n\} = \frac{2\pi}{\hbar S}\sum_{n',q_x,q_y}|\langle n'|e^{iq_y y}|n\rangle|^2|\langle 1|V_q(z)|1\rangle|^2 \times(2N_q+1)[f_{n'}(k_x+q_x)-f_n(k_x)] \times\delta\left(\epsilon_{n'}-\epsilon_n+\frac{\hbar^2}{2m}(q_x^2+2k_xq_x)\right). \quad (13)$$

The collision integral describing the scattering electrons by helium atoms in the gas phase can be obtained in a straightforward way from a similar collision integral derived by Saitoh[18] in the 2D case of SE's on helium. In the limit of $m/M_A \ll 1$, where M_A is the mass of the helium atom, it can be written as

$$\hat{S}_{eg}\{f_n\} = \frac{2\pi}{\hbar V^2}\sum_{n',q_x,\vec{\kappa},\kappa_y',\kappa_z'}|\eta_z(\kappa_z'-\kappa_z)|^2|\eta_y(\kappa_y'-\kappa_y)|^2 \times f_g(\kappa)[f_{n'}(k_x+q_x)-f_n(k_x)] \times\delta\left(\epsilon_{n'}-\epsilon_n+\frac{\hbar^2}{2m}(q_x^2+2k_xq_x)\right), \quad (14)$$

with

$$\eta_z(\kappa_z'-\kappa_z) = \sqrt{U_g}\int_0^\infty \chi_1^2(z)e^{i(\kappa_z'-\kappa_z)}\,dz$$

and

$$\eta_y(\kappa_y'-\kappa_y) = \sqrt{U_g}\int_{-\infty}^{\infty}\varphi_{n'}(y)\varphi_n(y)e^{i(\kappa_y'-\kappa_y)}dy,$$

where $U_g^2 = \pi\hbar^4 A/m^2$ is the strength of the electron-atom interaction, $A = 4.67\times10^{-16}$ cm^2 the effective cross section for this scattering, $f_g(\kappa) \propto \exp(-\hbar^2\kappa^2/2M_AT)$ the atom distribution function, and $\boldsymbol{\kappa}$ the wave vector of the helium atom. After some algebraic manipulations, Eq. (14) reduces to

$$\hat{S}_{eg}\{f_n\} = \frac{3\pi^2}{4}\frac{\hbar^3 n_g A\gamma}{m^2 L_x}\sum_{n',q_x}\langle\varphi_{n'}^2(y)\varphi_n^2(y)\rangle[f_{n'}(k_x+q_x) -f_n(k_x)]\delta\left(\epsilon_{n'}-\epsilon_n+\frac{\hbar^2}{2m}(q_x^2+2k_xq_x)\right) \quad (15)$$

where

$$\langle\varphi_{n'}^2(y)\varphi_n^2(y)\rangle = \int_{-\infty}^{\infty}[\varphi_{n'}(y)\varphi_n(y)]^2dy$$

and n_g is the volume concentration of the helium atoms in the gas phase. As one can see from Eqs. (13) and (15), both electron-ripplon scattering and electron-atom scattering are treated as elastic scattering in view of the absence of the scatter energy in the argument of the δ function. The reason for this in the case of electron-ripplon scattering was already pointed out. In the case of electron-atom scattering the condition $m/M_A \ll 1$ ensures that the scattering is elastic.

The Boltzmann equation, Eq. (10), can be solved in two limit situations depending on the contribution of the

electron-electron collision integral $\widehat{S}_{ee}\{f_n\}$. First, we will consider the case when the interelectron interaction is very weak and the corresponding collision integral can be omitted in Eq. (10). Second, if the frequency of electron-electron collision is high enough, $\widehat{S}_{ee}\{f_n\}$ plays a dominant role in the form of the distribution function. However, even in this limit, the electron-electron collisions can be taken into account in an indirect way without using any explicit form of $\widehat{S}_{ee}\{f_n\}$.

A. One-electron approximation

In this subsection we calculate the electron mobility within the one-electron approximation, when the electron-electron interaction is discarded in the solution of the Boltzmann equation and only the collision integrals due to electron-ripplon and electron-atom scatterings are retained in Eq. (10). As we are considering a quasi elastic process it is straightforward to write the distribution function in the following form within linear response theory:

$$f_n(k_x) = f_{0n}(|k_x|) + \frac{k_x}{|k_x|} f_{1n}(|k_x|). \tag{16}$$

Substituting Eq. (16) into Eq. (10), we can easily obtain the following expression for f_{1n}:

$$f_{1n} = -\frac{eE_{\|}}{\hbar[\nu_{er}^{(n)}(k_x) + \nu_{eg}^{(n)}(k_x)]} \frac{\partial f_{0n}}{\partial |k_x|}, \tag{17}$$

with

$$f_{0n} = \sqrt{\frac{2\pi\hbar^2}{mTL_x^2}} \frac{1}{Z_n} \exp\left[-\left(\frac{\hbar^2 k_x^2}{2mT} + \frac{\epsilon_n}{T}\right)\right] \tag{18}$$

and

$$Z_n = \sum_{n=0}^{\infty} \exp\left(-\frac{\epsilon_n}{T}\right) = \frac{1}{2} \exp\left(-\frac{\hbar\omega_0}{2T}\right) \left(1 + \coth\frac{\hbar\omega_0}{2T}\right),$$

where $\nu_{er}^{(n)}(k_x)$ [$\nu_{eg}^{(n)}(k_x)$] is the collision frequency for an electron in the nth subband with wave vector k_x due to electron-ripplon [electron-atom] scattering. These frequencies are given by

$$\nu_{er}^{(n)}(k_x) = \frac{2\pi}{\hbar S} \sum_{n', q_x, q_y} |\langle n'|e^{iq_y y}|n\rangle|^2 |\langle 1|V_q(z)|1\rangle|^2 \times (2N_q + 1) \left[1 - \frac{k_x(k_x + q_x)}{|k_x(k_x + q_x)|}\right] \times \delta\left(\epsilon_{n'} - \epsilon_n + \frac{\hbar^2}{2m}(q_x^2 + 2k_x q_x)\right) \tag{19}$$

and

$$\nu_{eg}^{(n)}(k_x) = \frac{3\pi^2}{4} \frac{\hbar^3 n_g A\gamma}{m^2 L_x} \sum_{n', q_x} \langle \varphi_{n'}^2(y)\varphi_n^2(y)\rangle \times \left[1 - \frac{k_x(k_x + q_x)}{|k_x(k_x + q_x)|}\right] \times \delta\left(\epsilon_{n'} - \epsilon_n + \frac{\hbar^2}{2m}(q_x^2 + 2k_x q_x)\right) \tag{20}$$

If we define the mean electron velocity along the x axis as

$$\langle v_x\rangle = \frac{\hbar}{m} \sum_{n, k_x} k_x f_n(k_x), \tag{21}$$

the electron mobility is given by $\mu = \langle v_x\rangle / E_{\|}$. From Eqs. (17), (18), and (21) it is easy to get the following expression for the electron mobility:

$$\mu = \frac{2e}{\sqrt{\pi} m Z_n} \left(\frac{\hbar\omega_0}{T}\right)^{\frac{3}{2}} \sum_{n=0}^{\infty} \exp\left(-\frac{\epsilon_n}{T}\right) \times \int_0^{\infty} dx \frac{\sqrt{x} e^{-\hbar\omega_0 x/T}}{\nu_{er}^{(n)}(x) + \nu_{eg}^{(n)}(x)}. \tag{22}$$

As one can see from Eq. (22), the collision frequencies are the quantities which determine the electron transport properties. For electron-ripplon scattering, the collision frequency can be written as

$$\nu_{er}^{(n)}(x) = \frac{4}{\sqrt{\pi}} \frac{e^2 E_{\perp}^2 T}{\alpha\hbar^2\omega_0\sqrt{x}} B_r^{(n)}(x), \tag{23}$$

with

$$B_r^{(n)}(x) = \frac{1}{16\sqrt{\pi}} \left\{ \int_0^{\infty} \frac{dy}{\sqrt{y}} e^{-4y} [L_n(4y)]^2 \left(\frac{1}{x+y} + \frac{8\sqrt{\hbar\omega_0\Delta_0}}{3\Delta_{\perp}} \frac{1}{\sqrt{x+y}} + \frac{16\hbar\omega_0\Delta_0}{9\Delta_{\perp}^2}\right) + \frac{1}{2} \sum_{n' \neq n}^{n'_{\max}} \frac{[\min(n', n)]!}{[\max(n', n)]!} \sqrt{\frac{x}{x + 4\beta_{nn'}}} \int_0^{\infty} dy (4y)^{|n'-n|-1/2} e^{-4y} \left[L_{\min(n', n)}^{|n'-n|}(4y)\right]^2 \times \left[\frac{4y + (\sqrt{x} - \sqrt{x + 4\beta_{nn'}})^2}{(y + \beta_{nn'})^2 + xy} + \frac{16\sqrt{\hbar\omega_0\Delta_0}}{3\Delta_{\perp}} \left(\frac{4y + (\sqrt{x} - \sqrt{x + 4\beta_{nn'}})^2}{(y + \beta_{nn'})^2 + xy}\right)^{1/2} + \frac{64\hbar\omega_0\Delta_0}{9\Delta_{\perp}^2}\right] \right\}, \tag{24}$$

where $x = \hbar^2 k_x^2/(2m\hbar\omega_0)$ is the electron kinetic energy normalized by $\hbar\omega_0$, $\beta_{nn'} = (n-n')/4$, $\Delta_0 = m\Lambda_0^2/2\hbar^2$, $\Delta_\perp = eE_\perp/\gamma$, $n'_{\max} = \mathrm{int}[n+x]$, $L_n^m(t)$ is the associated Laguerre polynomial, and $L_n(t) = L_n^0(t)$. In the above derivation we have used an approximate expression for the matrix elements of electron-ripplon scattering,

$$\langle 1|V_q(z)|1\rangle = \sqrt{\frac{\hbar q}{2\rho\omega_{rq}}}\left(\frac{\Lambda_0\gamma q}{3} + eE_\perp\right). \tag{25}$$

This approximation for $T \gtrsim 0.5$ K gives the value and the temperature dependence of SE mobility due to the polarization part of electron-ripplon scattering, described by the first term in Eq. (25), as compared with the results coming from using the exact interaction potential, given by Eq. (12).[19] This approximation was used, for example, in Ref. 15.

For electron-atom scattering, the collision frequency given by Eq. (20) can be reduced to

$$\nu_{eg}^{(n)}(x) = \frac{4}{\sqrt{\pi}}\frac{\hbar n_g A\gamma}{m\sqrt{x}} B_g^{(n)}(x), \tag{26}$$

with

$$B_g^{(n)}(x) = \frac{3\sqrt{\pi}}{2^{n+7/2}n!}\sum_{n'=0}^{n'_{\max}}\frac{1}{2^{n'}n'!}\sqrt{\frac{x}{x+4\beta_{nn'}}} \times \int_0^\infty \exp(-2y^2)\left[H_n(y)H_{n'}(y)\right]^2 dy\ . \tag{27}$$

Within the limit of $T \ll \hbar\omega_0$, only the lowest subband $n = 0$ participates in the transport process. The leading terms of the collision frequencies for ripplon and atom scattering are given by

$$\nu_{er}^{(0)} = \frac{e^2E_\perp^2 T}{4\alpha\hbar^2\omega_0 x}\exp(4x)\left[1-\mathrm{erf}(2\sqrt{x})\right] \tag{28}$$

and

$$\nu_{eg}^{(0)} = \frac{3\sqrt{\pi}\hbar n_g A\gamma}{8m\sqrt{x}}\ , \tag{29}$$

respectively, which reproduce the previous results in Ref. 12.

To make the problem more transparent, we have performed a numerical calculation for the collision frequencies. In the calculation, the temperature dependences of parameters α and n_g are determined by fitting experimental data.[20] α is in the range 0.34–0.375 erg/cm^2 for $T < 1.5$ and decreases with increasing temperature, and n_g is given by

$$n_g = n_0\exp(-\Delta E/T), \tag{30}$$

where $n_0 = 5.95\times10^{21}$/cm^3 and $\Delta E = 8.466$ K.

In Fig. 3, the collision frequencies $\nu_{er}^{(n)}$ of ripplon scattering of the first three subbands are depicted as a function of energy $E = \hbar^2k_x^2/2m + n\hbar\omega_0$ for $T = 0.6$ K and two different holding fields: $E_\perp$ =1000 V/cm and 3000 V/cm. We find that (i) the collision frequency decreases monotonously with increasing electron energy in the range $(n+1)\hbar\omega_0 > E > n\hbar\omega_0$; (ii) for the same energy E, the collision frequency increases with increasing the subband index n; and (iii) when the electron kinetic energy in the x direction equals the energy difference between two subbands $n\hbar\omega_0$, the collision frequency has a discontinuity jump. Each jump in the collision frequency corresponds to the threshold of a new scattering channel due to an intersubband interaction. For an electron in the lowest subband $n = 0$, only the intrasubband scattering is possible when its kinetic energy is less than $\hbar\omega_0$. For $x \to 0$, $\nu_{er}^{(0)} \propto x^{-1}(1-4\sqrt{x/\pi})$ and goes to infinity at the bottom of the subband where $x = 0$. When the electron kinetic energy is larger than $\hbar\omega_0$, intersubband scattering becomes possible and plays essential role in the scattering processes.

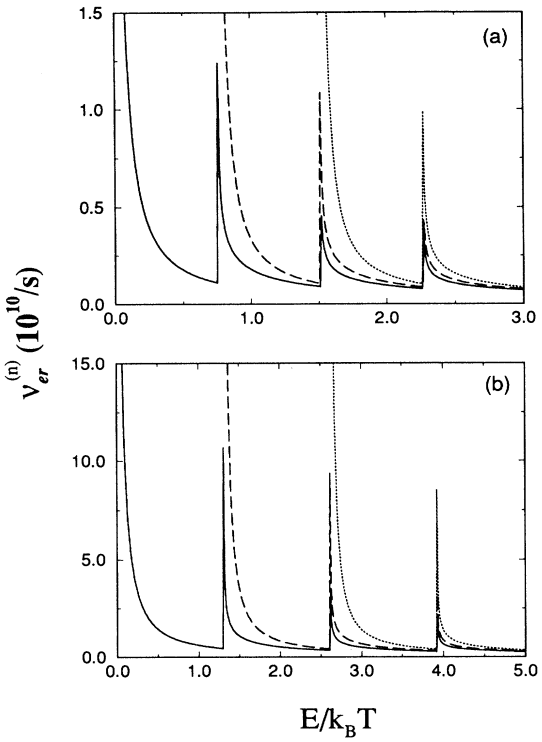

FIG. 3. The frequency of electron-ripplon collision as a function of energy $E = \hbar^2k_x^2/2m + n\hbar\omega_0$ for holding fields $E_\perp$=1000 V/cm and $E_\perp$=3000 V/cm at T =0.6 K. The solid, dashed, and dotted curves indicate n=0, 1, and 2, respectively.

Comparing Figs. 3(a) and 3(b), we observe that the collision frequencies at different holding fields have similar behavior. But, quantitatively, the scattering rate and the threshold of the intersubband scattering increase with increasing $E_\perp$. The collision frequency at $E_\perp$ = 3000 V/cm is about one order of magnitude larger than that at $E_\perp$ = 1000 V/cm.

In Fig. 4, the collision frequency $\nu_{eg}^{(n)}$ of atom scattering for the first three subbands is plotted as a function of energy $E = \hbar^2k_x^2/2m + n\hbar\omega_0$ at $T = 1.2$ K for the same set of holding fields: $E_\perp$ =1000 V/cm and 3000 V/cm. The behavior of the collision frequency for electron-atom scattering is similar as what was given in Fig. 3 for the electron-ripplon interaction. However, in the case of electron-atom scattering, the collision frequencies for the

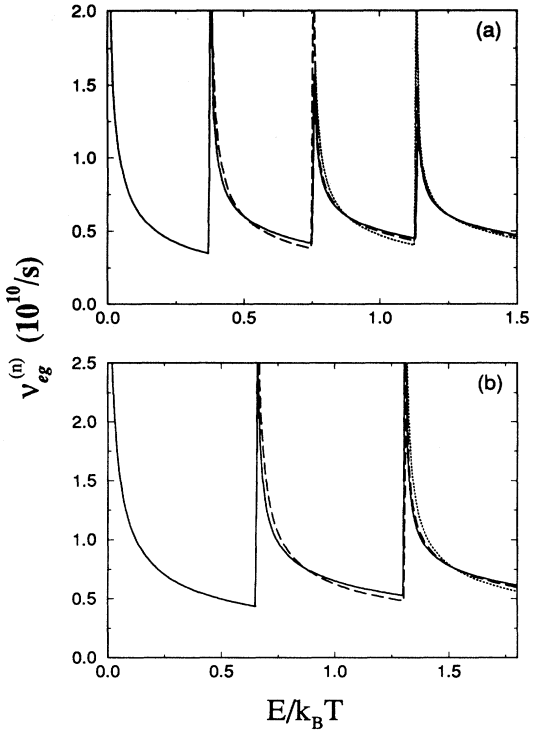

FIG. 4. The same as Fig. 3 but for the electron-atom collision frequency at $T = 1.2$ K.

electrons in different subbands are significantly closer to each other than in the case of electron-ripplon scattering and the collision frequency dependence on the holding field is very weak.

Note that a similar behavior of the collision frequency is found in other systems in which the processes of intrasubband and intersubband scattering are involved, like in 2D strongly δ-doped layers.[21]

From Eqs. (22), (23), and (26), the electron mobility can be written as

$$\mu = \frac{\mu_\perp (\hbar\omega_0/T)^{3/2}}{1+\coth(\hbar\omega_0/2T)} \sum_{n=0}^{\infty} \exp\left(-\frac{\hbar\omega_0}{T}n\right) \times \int_0^\infty \frac{x \exp\left(-\frac{\hbar\omega_0}{T}x\right) dx}{(T/\hbar\omega_0) B_r^{(n)}(x) + (\mu_\perp \hbar n_g A\gamma/e)\, B_g^{(n)}(x)}, \tag{31}$$

where $B_r^{(n)}(x)$ and $B_g^{(n)}(x)$ are given by Eqs. (24) and (27), respectively, and

$$\mu_\perp = \frac{\alpha\hbar}{meE_\perp^2} . \tag{32}$$

At $T \to 0$, the electron mobility is given by

$$\mu_{er}^{(0)} = 6\mu_\perp , \tag{33}$$

due to the collision frequency in Eq. (28). In the regime of electron-gas scattering and in the limit of $\hbar\omega_0 \gg T$, by using Eq. (29), the mobility can be written as

$$\mu_{eg}^{(0)} = \frac{16}{3\pi} \frac{e}{\hbar n_g A\gamma} \left(\frac{T}{\hbar\omega_0}\right)^{1/2} . \tag{34}$$

In Fig. 5(a), the electron mobility is plotted as a function of temperature for different holding fields. The mobility normalized by $\mu_\perp$ is given in Fig. 5(b), and the calculated mobility including only electron-ripplon (thin-dashed curves) or electron-atom (thin-dotted curves) scattering is shown to illustrate the importance of the respective mechanisms in different temperature regions. It is interesting to observe that, despite the complicated structure of the energy dependence of $\nu_{er}^{(n)}$ and $\nu_{eg}^{(n)}$, the mobility is still a smooth curve as a function of temperature. When $T \to 0$, $\mu/\mu_\perp \to 6$ which is consistent with Eq. (33). One can see that for temperatures below 0.8 K, electron-ripplon scattering dominates the mobility which has a stronger temperature dependence under small hold-

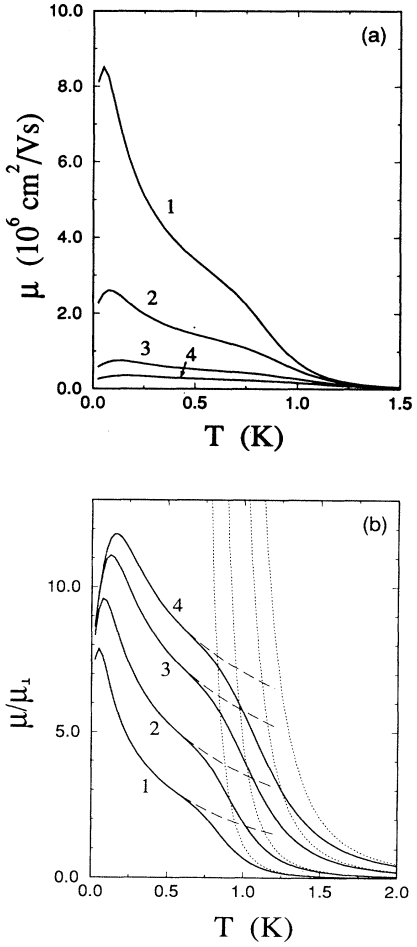

FIG. 5. (a) The electron mobility within the one-electron approximation as a function of temperature. The mobility is normalized by $\mu_\perp = \alpha\hbar/meE_\perp^2$ in (b), and the dashed (dotted) curves present the mobility including ripplon (gas) scattering only. The curves numbered 1–4 correspond to $E_\perp$ = 500, 1000, 2000, and 3000 V/cm, respectively.

ing fields, and for $T \gtrsim 1.0$ K the electron mobility is determined by electron-atom scattering where the mobility decreases exponentially with increasing temperature. For the temperature in between, both scattering mechanisms are important. Notice that, because $\mu_\perp \propto E_\perp^{-2}$, the normalized mobility in Fig. 5(b) increases with increasing $E_\perp$, while for the mobility depicted in Fig. 5(a), we found an opposite behavior.

We also observe that a maximum of μ appears at $T < 0.2$ K for the holding fields considered. At such low temperatures, the electron mobility is entirely dominated by ripplon scattering and the origin of the maximum should be explained by Eqs. (22), (23), and (31) without considering gas scattering. It is clear from Eqs. (22) and (31) that electrons which have a normalized kinetic energy $x \lesssim T/\hbar\omega_0$ are important for the mobility due to the factor $\exp(-\hbar\omega_0 x/T)$ in the integrand. In the limit of low temperature $T \ll \hbar\omega_0$, when the contribution of very small x is essential in these equations, only electrons in the lowest subband $n = 0$ contribute to the transport and the leading term of the collision frequency is given by Eq. (28), which gives $\mu = 6\mu_\perp$ at $T \to 0$. By expanding Eq. (31) in a power series, considering only $x \ll 1$, and neglecting $B_g^{(n)}$ in the denominator, we can easily obtain the following expression for the mobility, which describes its behavior as the temperature starts to increase from zero:

$$\mu = \mu_{er}^{(0)} \left[1 + \frac{32}{3\pi}\left(\frac{T}{\hbar\omega_0}\right)^{1/2}\right]. \tag{35}$$

Equation (35) shows explicitly the increase of the mobility from its limiting value $\mu_{er}^{(0)} = 6\mu_\perp$ which is observed in Figs. 5(a) and 5(b) at low temperatures. When the temperature is comparable or higher than $\hbar\omega_0$, the condition $x \ll 1$ in Eq. (31) becomes unsatisfactory and Eq. (35), obtained in the limit $T \ll \hbar\omega_0$, is not valid. At higher temperatures, the value of the mobility can be only obtained numerically through Eqs. (31), (24), and (27). The results of these calculations, depicted in Figs. 5(a) and 5(b), demonstrate the decrease of the mobility with increasing temperature when both the intersubband transitions and the increase of the population of electrons in subbands with $n > 0$ become dominant. So, due to these different behaviors, a maximum in the mobility takes place. Since the higher is the holding field, the larger is the subband separation $\hbar\omega_0$, we observe that the interval of temperature, where the contribution to the mobility coming from electrons in the subband $n = 0$, [Eq. (35)], becomes larger. As a consequence, the position of the maximum of the mobility shifts to higher temperatures with increasing the holding field. On the other hand, the strength of the electron-ripplon interaction increases and the effective width y_0 decreases with the increase of $E_\perp$. Furthermore, the collision frequency increases as is shown in Fig. 3 and the electron mobility decreases.

B. Complete control approximation

In this section the Boltzmann equation, Eq. (10), will be solved in the limit when the frequency of the electron-electron collisions, ν_{ee}, is much larger than the typical frequencies $\nu_{er}^{(n)}$ and $\nu_{eg}^{(n)}$. This situation for SE's over a flat helium surface is realized in a definite range of electron densities, as shown in Ref. 15. As is well known, the electron density can be easily varied by changing the holding field $E_\perp$ in the case of SE's. The conditions necessary to realize a similar situation, the so-called complete control regime, in the Q1D system are not so clear at the present time in view of the anisotropic character of the electron motion and a more complicated dependence of the electron density on the holding field. This issue has not been solved in the general case up to now. However, we expect that the complete control approximation should describe the main features of the electron transport in the Q1D channels.

In the complete control approximation the distribution function f_n is represented by

$$f_n = f_{n0} + f_{n1} , \tag{36}$$

where f_{n0} satisfies Eq. (10) in such a way that $\nu_{ee} \gg \nu_{er}^{(n)}$ and $\nu_{eg}^{(n)}$. In this case, we have in zero-order approximation

$$\widehat{S}_{ee}\{f_{n0}\} = 0 . \tag{37}$$

The solution of Eq. (37) gives

$$f_{n0} = \sqrt{\frac{2\pi\hbar^2}{mTL_x^2}}\frac{1}{Z_n}\exp\left[-\left(\frac{\hbar^2 k_x^2}{2mT} + \frac{\epsilon_n}{T}\right) + \frac{\hbar u k_x}{T}\right] . \tag{38}$$

The drift electron velocity along the driving field u can be calculated from the Boltzmann equation if we multiply both sides of Eq. (10) by k_x and sum over n and k_x. The procedure is similar to what was used in Ref. 15. As a result, the mobility $\tilde{\mu} = u/E_\parallel$ can be written as

$$\tilde{\mu} = \frac{e}{m(\tilde{\nu}_{er} + \tilde{\nu}_{eg})} , \tag{39}$$

where

$$\tilde{\nu}_{er(eg)} = -\frac{\hbar}{mu}\sum_{n,k_x} k_x \widehat{S}_{er(eg)}\{f_{n0}\} \tag{40}$$

is the average collision frequency due to electron-ripplon (electron-atom) scattering.

Substituting Eq. (13) into Eq. (40), we obtain the following expressions for the collision frequency of ripplon scattering:

$$\tilde{\nu}_{er} = \frac{e^2E_\perp^2}{\alpha\hbar}\left[1 + \coth\left(\frac{\hbar\omega_0}{2T}\right)\right]^{-1} \times \sum_{n,n'} \exp\left(-\frac{\hbar\omega_0(n+n')}{2T}\right) D_{nn'}^{(r)}(T), \tag{41}$$

where

$$D_{nn'}^{(r)} = 2\sqrt{\frac{\hbar\omega_0}{\pi^3 T}}\frac{[\min(n,n')]!}{[\max(n,n')]!}\int_0^\infty dy\,(4y)^{|n-n'|-1/2}e^{-4y}\left[L_{\min(n,n')}^{|n-n'|}(4y)\right]^2$$
$$\times\left\{\int_0^\infty \frac{\exp[-(x+\beta_{nn'}^2/x)\hbar\omega_0/T]}{x+y}dx + \frac{8(\hbar\omega_0\Delta_0)^{1/2}}{3\Delta_\perp}\int_0^\infty \frac{\exp[-(x+\beta_{nn'}^2/x)\hbar\omega_0/T]}{\sqrt{x+y}}dx\right.$$
$$\left.+\frac{32\hbar\omega_0\Delta_0}{9\Delta_\perp^2}|\beta_{nn'}|\,K_1(|\beta_{nn'}|\hbar\omega_0/T)\right\}, \tag{42}$$

and for $n = n'$,

$$D_{nn}^{(r)} = \frac{1}{\pi^{3/2}}\int_0^\infty \exp\left[\left(1-\frac{4T}{\hbar\omega_0}\right)y\right]\left[L_n\left(\frac{4Ty}{\hbar\omega_0}\right)\right]^2$$
$$\times\left\{E(y) + \frac{8\sqrt{\pi}}{3}\frac{(\Delta_0 T)^{1/2}}{\Delta_\perp}[1-\mathrm{erf}(\sqrt{y})]\right.$$
$$\left.+\frac{16}{9}\frac{\Delta_0 T}{\Delta_\perp^2}\exp(-y)\right\}\frac{dy}{\sqrt{y}}, \tag{43}$$

where $E(y) = -Ei(-y)$ is the exponential-integral function and the other notations are the same as in Eq. (24).

From Eqs. (40) and (15), we obtain the collision frequency of electron-atom scattering,

$$\tilde{\nu}_{eg} = \frac{\hbar n_g A\gamma}{m}\left(\frac{\hbar\omega_0}{T}\right)^{\frac{1}{2}}\left[1+\coth\left(\frac{\hbar\omega_0}{2T}\right)\right]^{-1}$$
$$\times\sum_{n,n'}\exp\left(-\frac{\hbar\omega_0(n+n')}{2T}\right)D_{nn'}^{(g)}(T)\ , \tag{44}$$

where

$$D_{nn'}^{(g)} = \frac{6\sqrt{2}|\beta_{nn'}|\hbar\omega_0}{\sqrt{\pi}n!n'!2^{n+n'}T}K_1(2|\beta_{nn'}|\hbar\omega_0/T)$$
$$\times\int_0^\infty [H_n(x)H_{n'}(x)]^2\exp(-2x^2)dx\ , \tag{45}$$

and for $n = n'$,

$$D_{nn}^{(g)} = \frac{3\sqrt{2}}{\sqrt{\pi}(n!2^n)^2}\int_0^\infty [H_n(x)]^4\exp(-2x^2)dx. \tag{46}$$

Substituting Eqs. (41) and (44) into Eq. (39), the result of the electron mobility is

$$\tilde{\mu} = \mu_\perp[1+\coth(\hbar\omega_0/2T)]$$
$$\times\left[G_r + \frac{\mu_\perp\hbar n_g A\gamma}{e}\left(\frac{\hbar\omega_0}{T}\right)^{\frac{1}{2}}G_g\right]^{-1}\ , \tag{47}$$

where

$$G_{r(g)} = \sum_{n,n'}\exp\left(-\frac{\hbar\omega_0(n+n')}{2T}\right)D_{nn'}^{r(g)}\ . \tag{48}$$

The limiting values of mobilities in the regions of electron-ripplon and electron-gas scattering at $\hbar\omega_0 \gg T$ are given by

$$\tilde{\mu}_{er}^{(0)} = 2\mu_\perp \tag{49}$$

and

$$\tilde{\mu}_{eg}^{(0)} = \frac{4e}{3\hbar n_g A\gamma}\left(\frac{T}{\hbar\omega_0}\right)^{1/2}\ . \tag{50}$$

The mobility $\tilde{\mu}$ within the complete control approximation is shown as a function of temperature for different holding fields in Fig. 6(a). It is seen that the temperature dependence of the mobility is qualitatively similar to that in Fig. 5(a) within the one-electron approximation. However, the results in Fig. 6(a) demonstrate the peculiarities

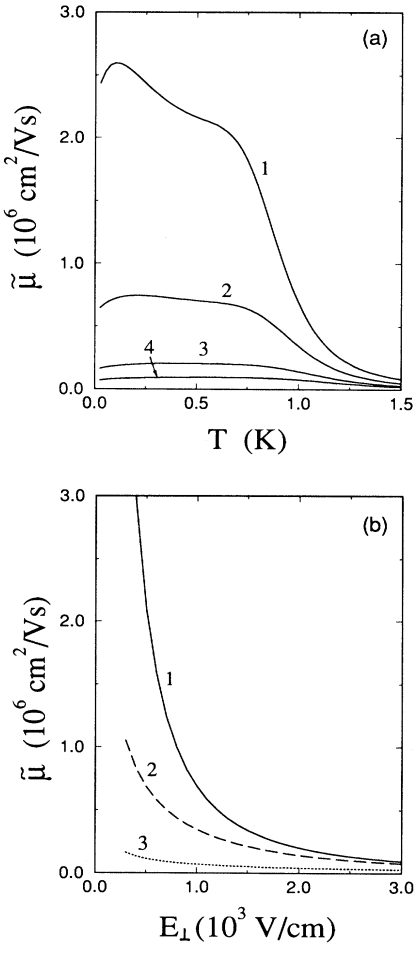

FIG. 6. The electron mobility within the complete control approximation as a function of (a) the temperature with different holding fields $E_\perp$ = 500, 1000, 2000, and 3000 V/cm, corresponding to the curves numbered 1–4 and (b) the holding field with T = 0.6, 1.0, and 1.4 K, corresponding to the curves numbered 1–3.

which make them different from Fig. 5(a). First, in the temperature region $T \lesssim 0.8$ K, where ripplon scattering is the dominating scattering mechanism, the mobility is a factor of 2–3 smaller than that within the one-electron approximation. At $T \to 0$, this factor goes to 3 which agrees with the analytical results $\mu_{er}^{(0)}$ and $\tilde{\mu}_{er}^{(0)}$ given by Eqs. (33) and (49). In the regime where gas scattering dominates the mobility, $T \gtrsim 1.0$ K, the result in the one-electron approximation is slightly larger than that in the complete control approximation. Their ratio $\mu_{eg}^{(0)}/\tilde{\mu}_{eg}^{(0)}$, from Eqs. (34) and (50), is close to $4/\pi$ for $\hbar\omega_0 \gg T$. Second, $\tilde{\mu}$ has a maximum at low temperature due to a similar reason as discussed in the above subsection. Indeed, at $T \to 0$ and when electron-ripplon scattering is dominant, the mobility is entirely determined from the contribution of the subband $n = 0$. With this condition, the temperature dependence of the mobility, given by Eq. (47), is determined by the function $G_r \simeq D_{00}^{(r)}(T)$. By calculating the asymptotic limit of $D_{00}^{(r)}(T)$, given by Eq. (43), for $T/\hbar\omega_0 \ll 1$, we obtain the following expression for the mobility:

$$\tilde{\mu} = \tilde{\mu}_{er}^{(0)} \left[1 + \frac{4}{\pi} \left(\frac{T}{\hbar\omega_0} \right)^{1/2} \right]. \tag{51}$$

The increase of the mobility, shown in Fig. 6(a), from its limiting value $\tilde{\mu}_{er}^{(0)} = 2\mu_\perp$, agrees with the result in Eq. (51) and is qualitatively similar to the behavior of the mobility in the one-electron approximation [see Eq. (35)]. As in the case of the one-electron approximation, the influence of the intersubband transitions and the growth of the population of the subbands with $n > 0$, which become essential at $T \sim \hbar\omega_0$, lead to the decrease of $\tilde{\mu}$ with the appearance of a maximum at an intermediate temperature. However, the numerical factor in the second term of Eq. (51) is 8/3 times smaller than that in Eq. (35). Because of this fact, the mobility $\tilde{\mu}$ increases more slowly in compared with μ and the position of the peak shifts to higher temperature compared with that of the one-electron approximation result. For $E_\perp =$ 500, 1000, 2000, and 3000 V/cm, the peaks appear at $T = 0.12$, 0.21, 0.41, and 0.57 K, respectively.

Figure 6(b) shows the mobility within the complete control approximation as a function of holding field for three temperatures related to electron-ripplon (0.6 K) and electron-gas (1.4 K) scattering, as well as for an intermediate temperature (1.0 K). We find that, at $T = 0.6$ K, $\tilde{\mu} \sim E_\perp^{-1.9}$ for $E_\perp > 1000$ V/cm and has a very weak dependence at $T = 1.4$ K. For the 2D electron system over a flat helium surface, the field dependence in the regime of ripplon scattering is $\mu \sim E_\perp^{-2}$ for high enough holding fields.[16] In the gas scattering regime the field dependence of the mobility is very weak, being entirely determined by the field dependence of the parameter γ, which describes the scale of the electron localization along the z direction. Therefore, the field dependences of the mobility in both SE's over bulk helium and in the Q1D charge channel filled by helium are similar despite the more complicated structure of the expressions in the case of the Q1D electron system.

For the sake of comparison, we present in Fig. 7(a) the mobilities within the two different approximations by considering only electron-ripplon scattering and in Fig. 7(b) the results in the case of electron-gas scattering. As one can see from Fig. 7(a) the mobility in the one-electron approximation $\mu(T)$ shows a stronger dependence in the region of electron-ripplon scattering as compared with the mobility in the complete control approximation $\tilde{\mu}(T)$. For $E_\perp = 1000$ V/cm, the ripplon-limited mobility behaves as $\mu(T) \sim T^{-0.5}$ in the interval $0.4 < T < 0.7$ K. For $E_\perp = 500$ V/cm, as shown in Fig. 5(a), $\mu(T) \sim T^{-1}$. For the same values of the holding fields the mobility $\tilde{\mu}(T)$ has a weaker temperature dependence, as shown in Figs. 6(a) and 7(a). One should remember that for SE's in the 2D case, the dependence $\mu(T) \sim T^{-1}$ is observed only in the limit $E_\perp \to 0$ and for temperatures in the interval 0.5–0.7 K,[19,22] and this dependence is significantly weaker for holding fields in the range 10^2–10^3 V/cm.

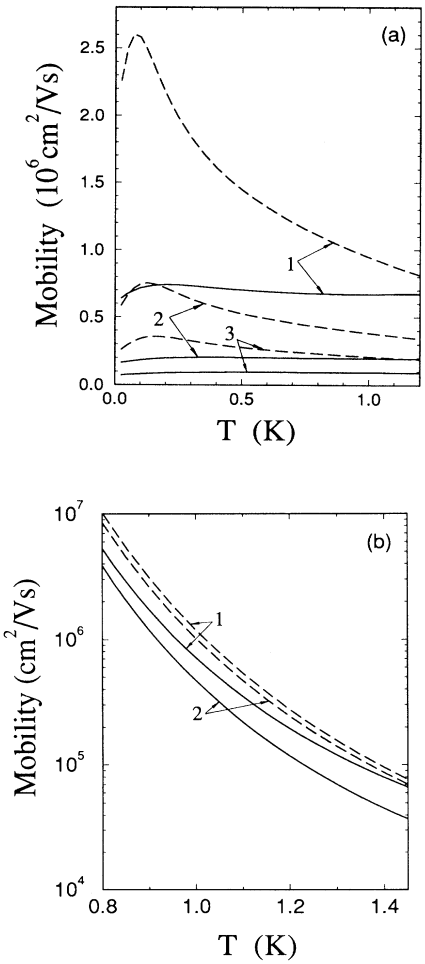

FIG. 7. The contributions of (a) the electron-ripplon and (b) electron-gas scattering to mobilities within the one-electron approximation (dashed curves) and the complete control approximation (solid curves) for holding fields $E_\perp = 1000$, 2000, and 3000 V/cm numbered 1–3.

The maximum of the mobility within the one-electron approximation appears at $T < 0.2$ K for the holding fields under consideration. However, the approximation for the electron-ripplon interaction given in Eq. (25) becomes invalid at low temperatures. In addition, one cannot exclude the possibility of the transition of the electron system in the quasiordered state[11] at very low temperature. Under such a transition, the possibility of the description of the electron system in the framework of standard kinetic approach disappears. So the present theory intends to describe the electron mobility correctly for $T \gtrsim 0.4$–0.5 K where $\mu(T)$ is a monotonous function of the temperature. In contrast, the peak in the mobility calculated in the complete control approximation occurs at $T > 0.4$ K for $E_\perp > 2000$ V/cm and at $T = 0.57$ K for $E_\perp = 3000$ V/cm, where the present theory gives a reliable description of electron-ripplon scattering.

For SE's over a flat liquid helium surface, the temperature dependences of the mobility within the one-electron and the complete control approximation are similar qualitatively, but the mobility within the one-electron approximation is 2 times higher at high enough electric fields in the regime of electron-ripplon scattering.[15,23] The reason for such a discrepancy, explained in Refs. 15 and 23, is due to the strong dependence of the electron-ripplon collision frequency on electron momentum at large holding fields. The dependence of the collision frequency on the electron momentum is of fundamental importance to the calculation of the mobility either in the one-electron case (the average of the inverse frequency) or in the complete control case (the average of the frequency). Due to this, the mobility in these two regimes differs quantitatively in the two-dimensional case at large $E_\perp$. At the same time, the momentum dependence of the electron-ripplon collision frequency disappears at $E_\perp \to 0$ and the mobilities in such a case are the same in both the one-electron regime and in the complete control regime with a strong role of interelectron correlations.

In the present Q1D system, the strong dependence of the electron-ripplon collision frequency, on the momentum k_x through x in Eq. (24), takes place for both the contributions from the holding field and the polarization part of the electron-ripplon interaction [the first term in Eq. (25)]. Due to this dependence, the discrepancy in the mobilities obtained in the two different approximations is more fundamental than that in the 2D case, demonstrating the more essential role of interelectron correlations in reducing the dimensionality of the system. Moreover, the dependence of the electron-gas collision frequency in Eqs. (26) and (27) on the electron momentum leads to a difference between μ and $\tilde{\mu}$ in the regime of electron-gas scattering for $T > 1$ K [see Fig. 7(b)], contrary to the 2D case, where the electron-gas collision frequency is independent of the momentum and the two approximations yield the same temperature dependence of the mobility.[15]

IV. CONCLUSIONS

We calculated the electron mobility in the Q1D charge channel filled with liquid helium. The results are obtained within two approximations. One of them is the one-electron approximation in which the electron-electron interaction can be neglected and the other one is the complete control approximation within which the electron-electron correlations influence strongly the structure of the electron distribution function. The temperature dependence of the mobility calculated in both approximations shows a nonmonotonic behavior with the appearance of a maximum at a certain temperature, in contrast to the monotonous temperature dependence of the mobility in the 2D case taking into account the same scattering mechanisms.[15,16,18,19] Then, we can conclude that the nonmonotonic behavior of the mobility is attributed to the specific nature of the electron motion in the Q1D charge motion. The position of the maximum is different in both approximations. If the complete control regime is realized in the Q1D charge channel over liquid helium, the maximum in the temperature dependence of the mobility will appear at a temperature near 0.5 K. The experimental observation of the nonmonotonic temperature dependence of the electron mobility around this temperature can give evidence of the applicability of the complete control approximation in the description of the electron kinetics in the Q1D charge channel in addition to the SE's over a flat helium surface where the complete control regime was shown to be realized.[15,23] The mobility calculated in the complete control approximation is near 3 times lower than that in the one-electron approximation within the temperature range where electron-ripplon scattering is dominant and this difference is smaller in the regime where electron-gas scattering dominates. For the sake of comparison, in the case of SE's over bulk helium, the mobility in the regime of ripplon scattering calculated in the one-electron approximation is 2 times higher than that in the complete control approximation and in the regime of gas scattering both approximations give the same results. The field dependence of the mobility exhibits the power law $\mu \sim E_\perp^{-1.9}$ in the regime of electron-ripplon scattering and a weak dependence on $E_\perp$ in the regime of electron-gas scattering.

Up to now, the only experimental study, as far as we know, of the electron conductivity in the Q1D electron system on liquid helium was carried out in Ref. 14. In this work the dependence of electron conductivity on the holding potential was measured. The result shows a sharp nonmonotonic dependence on the holding potential, not only for the electron conductivity, but also for the charge concentration in the channel. In addition, the experimental results depend crucially on the conditions of electron charging of the Q1D channel. As a consequence, we cannot compare directly our calculations with the results of Ref. 14, even though the decrease of the observed conductivity with increasing the holding potential, when the helium surface is charged at zero holding potential, follows directly from the results of the present work. For a detailed comparison of our theory, we need experiments in which the electron density should be fixed or at least changes according to some known law. The results of such experimental studies, especially, the temperature dependence of the electron mobility, together with the present calculations, can check not only the role of the electron confinement in the Q1D channel, but also the

representations available for the scattering mechanisms and the possible influence of interelectron correlations on the electron transport in this channel.

ACKNOWLEDGMENTS

This work was partially sponsored by the Fundação de Amparo à Pesquisa do Estado de São Paulo (FAPESP) and the Conselho Nacional de Desenvolvimento Científico e Tecnológico (CNPq). One of us (S.S.S.) is grateful to FAPESP for financial support and to the B. I. Verkin Institute for Low Temperature Physics and Engineering, Kharkov, for a leave of absence. G.Q.H. is supported by CNPq, Brazil.

[1]T. Ando, A. B. Fowler, and F. Stern, Rev. Mod. Phys. **54**, 437 (1982); M. J. Kelly and R. J. Nicholas, Rep. Prog. Phys. **48**, 1699 (1985); G. Bastard, J. A. Brum, and R. Ferreira, in *Solid State Physics*, edited by H. Ehrenreich, F. Seitz, and D. Turnbull (Academic Press, New York, 1991), Vol. 44, p. 229.

[2]M. W. Cole, Rev. Mod. Phys. **46**, 451 (1974); Yu. P. Monarkha and V. B. Shikin, Fiz. Nizk. Temp. **8**, 563 (1982) [Sov. J. Low Temp. Phys. **8**, 279 (1982)]; F. I. B. Williams, Surf. Sci. **113**, 371 (1982); N. Studart and O. Hipólito, Rev. Bras. Fis. **16**, 194 (1986); P. Leiderer, J. Low Temp. Phys. **87**, 247 (1992).

[3]C. W. J. Beenakker and H. van Houten, in *Solid State Physics*, edited by H. Ehrenreich and D. Turnbull (Academic, New York, 1991), Vol. 44, p. 1; G. Timp, R. Behringer, S. Sampere, J. E. Cunningham, and R. E. Howard, in *Nanostructure Physics and Fabrication*, edited by M. A. Reed and W. P. Kirk (Academic, San Diego, 1989), p. 331.

[4]A. S. Plaut, H. Lage, P. Grambow, D. Heitmann, K. von Klitzing, and K. Ploog, Phys. Rev. Lett. **67**, 1642 (1991); T. Egeler, G. Abstreiter, G. Weimann, T. Demel, D. Heitmann, and W. Schlapp, *ibid.* **65**, 1804 (1990); Y. Nagamune, Y. Arakawa, S. Tsukamoto, M. Nishioka, S. Sasaki, and N. Miura, *ibid.* **69**, 2963 (1992).

[5]M. Tewordt, V. J. Law, M. J. Kelly, R. Newbury, M. Pepper, D. C. Peacock, J. E. F. Frost, D. A. Ritchie, and G. A. C. Jones, J. Phys. C **2**, 8969 (1990); S. Tarucha, Y. Hirayama, T. Saku, and T. Kimura, Phys. Rev. B **41**, 5459 (1990); P. E. F. Farinas, G. E. Marques, and N. Studart, in *Proceedings of the 21st International Conference on the Physics of Semiconductors*, edited by P. Jiang and H.-Z. Zheng (World Scientific, Singapore, 1992), Vol. 1, p. 657.

[6]B. Y.-K. Hu and S. Das Sarma, Phys. Rev. Lett. **68**, 1750 (1992); L. Wendler and V. G. Grigoryan, Phys. Rev. B **49**, 14 531 (1994); I. Grodnensky, D. Heitmann, K. von. Klitzing, K. Ploog, A. Rudenko, and A. Kamaev, *ibid.* **49**, 10 778 (1994).

[7]G. Weber, P. A. Schulz, and L. E. Oliveira, Phys. Rev. B **38**, 2179 (1988); A. Ferreira da Silva, *ibid.* **41**, 1684 (1990).

[8]G. Q. Hai, F. M. Peeters, J. T. Devreese, and L. Wendler, Phys. Rev. B **48**, 12 016 (1993); V. B. Campos and S. Das Sarma, *ibid.* **49**, 1867 (1992); G. Fishman, *ibid.* **36**, 7448 (1987); B. K. Ridley, Rep. Prog. Phys. **54**, 169 (1991).

[9]Vl. L. Ginzburg and Yu. P. Monarkha, Fiz. Nizk. Temp. **4**, 1236 (1978) [Sov. J. Low Temp. Phys. **4**, 580 (1978)].

[10]Yu. Z. Kovdrya, F. F. Mende, and V. A. Nikolaenko, Fiz. Nizk. Temp. **10**, 1129 (1984) [Sov. J. Low Temp. Phys. **10**, 589 (1984)].

[11]A. V. Chaplik, Pis'ma Zh. Eks. Teor. Fiz. **31**, 275 (1980) [JETP Lett. **31**, 252 (1980)].

[12]Yu. V. Kovdrya and Yu. Monarkha, Fiz. Nizk. Temp. **12**, 1011 (1986) [Sov. J. Low Temp. Phys. **2**, 571 (1986)].

[13]Yu. V. Kovdrya and V. A. Nikolaenko, Fiz. Nizk. Temp. **18**, 1278 (1992) [Sov. J. Low Temp. Phys. **18**, 894 (1992)].

[14]O. I. Kirichek, Yu. P. Monarkha, Yu. Z. Kovdrya, and V. N. Grigor'ev, Fiz. Nizk. Temp. **19**, 458 (1993) [Sov. J. Low Temp. Phys. **19**, 323 (1993)].

[15]V. A. Buntar', V. N. Grigoriev, O. I. Kirichek, Yu. Z. Kovdrya, Yu. P. Monarkha, and S. S. Sokolov, J. Low Temp. Phys. **79**, 323 (1990).

[16]V. B. Shikin and Yu. P. Monarkha, J. Low Temp. Phys. **16**, 193 (1974).

[17]M. C. Pereira, G. E. Marques, and N. Studart, Phys. Rev. B **46**, 1857 (1992); Yu. P. Monarkha, S. S. Sokolov, and V. B. Shikin, Solid State Commun. **38**, 611 (1980).

[18]M. Saitoh, J. Phys. Soc. Jpn. **42**, 201 (1977).

[19]Yu. P. Monarkha, Fiz. Nizk. Temp. **2**, 1232 (1976) [Sov. J. Low Temp. Phys. **2**, 600 (1976)].

[20]B. N. Esel 'son, V. N. Grigor 'ev, V. G. Ivantsov, and E. Ya. Rudavskii, *Properties of Liquid and Solid Helium* (Izdatel'stvo Standartov, Moscow, 1978).

[21]G. Q. Hai, F. M. Peeters, J. T. Devreese, and N. Studart (unpublished).

[22]B. N. Esel'son, A. S. Rybalko, and S. S. Sokolov, Fiz. Nizk. Temp. **6**, 1120 (1980) [Sov. J. Low Temp. Phys. **6**, 544 (1980)].

[23]V. A. Buntar', Yu. Z. Kovdrya, V. N. Grigoriev, Yu. P. Monarkha, and S. S. Sokolov, Fiz. Nizk. Temp. **13**, 789 (1987) [Sov. J. Low Temp. Phys. **13**, 451 (1987)].